Velocity autocorrelation by quantum simulations for direct parameter-free computations of the neutron cross sections. II. Liquid deuterium

E. Guarini,[1] M. Neumann,[2] U. Bafile,[3] M. Celli,[3] D. Colognesi,[3] S. Bellissima,[1] E. Farhi,[4] and Y. Calzavara[4]
[1]*Dipartimento di Fisica e Astronomia, Università degli Studi di Firenze, via G. Sansone 1, I-50019 Sesto Fiorentino, Italy*
[2]*Fakultät für Physik der Universität Wien, Strudlhofgasse 4, A-1090 Wien, Austria*
[3]*Consiglio Nazionale delle Ricerche, Istituto dei Sistemi Complessi, via Madonna del Piano 10, I-50019 Sesto Fiorentino, Italy*
[4]*Institut Laue-Langevin, 71 avenue des Martyrs, CS 20156, F-38042 Grenoble Cedex 9, France*
(Received 9 January 2016; revised manuscript received 15 April 2016; published 13 June 2016)

Very recently we showed that quantum centroid molecular dynamics (CMD) simulations of the velocity autocorrelation function provide, through the Gaussian approximation (GA), an appropriate representation of the single-molecule dynamic structure factor of liquid H_2, as witnessed by a straightforward absolute-scale agreement between calculated and experimental values of the total neutron cross section (TCS) at thermal and epithermal incident energies. Also, a proper quantum evaluation of the self-dynamics was found to guarantee, via the simple Sköld model, a suitable account of the distinct (intermolecular) contributions that influence the neutron TCS of para-H_2 for low-energy neutrons (below 10 meV). The very different role of coherent nuclear scattering in D_2 makes the neutron response from this liquid much more extensively determined by the collective dynamics, even above the cold neutron range. Here we show that the Sköld approximation maintains its effectiveness in producing the correct cross section values also in the deuterium case. This confirms that the true key point for reliable computational estimates of the neutron TCS of the hydrogen liquids is, together with a good knowledge of the static structure factor, the modeling of the self part, which must take into due account quantum delocalization effects on the translational single-molecule dynamics. We demonstrate that both CMD and ring polymer molecular dynamics (RPMD) simulations provide similar results for the velocity autocorrelation function of liquid D_2 and, consequently, for the neutron double differential cross section and its integrals. This second investigation completes and reinforces the validity of the proposed quantum method for the prediction of the scattering law of these cryogenic liquids, so important for cold neutron production and related condensed matter research.

DOI: 10.1103/PhysRevB.93.224302

I. INTRODUCTION

Experimental and computational investigations of the physical properties of light molecular liquids such as H_2 and D_2 are topical subjects of intense research work. The reasons for this interest are manifold, since disparate fields of research would greatly benefit from progresses in the understanding of these liquids: from the formulation of appropriate quantum theories, to the prediction of their behavior on other planets, to, finally, well-known applications related to energy storage, cryogenics, and neutron moderation for condensed matter spectroscopic studies. Theoretical, computational, and technical challenges posed by the hydrogen liquids all stem from their "mild" quantum nature that places these two liquids midway between the case of liquid He and that of classical fluids. This means that most of their properties can be deduced by treating the molecules still as Boltzmann (distinguishable) particles, but there is no way that classical methods will be able to reproduce the experimental reality. For instance, Monte Carlo and molecular dynamics simulations aimed at predicting the structural and dynamical properties of H_2 and D_2 at liquid temperatures must be generalized to model, in an effective way, the occurrence of particle quantum delocalization, as accomplished by the path-integral Monte Carlo (PIMC) method [1] and by techniques like centroid molecular dynamics (CMD) [2,3] and ring polymer molecular dynamics (RPMD) [4–6].

As far as the static and dynamic structural properties of condensed systems are concerned, a strong coupling has always existed between liquid hydrogens and neutron spectroscopy, since they are mutually very important for each other. Indeed neutrons are the ideal probe for spectroscopic investigations, at the nanometer and picosecond length and time scales, of light elements. Moreover, neutrons are scattered in a very different way by the two hydrogen isotopes, making isotopic substitution in neutron experiments a very effective method to access either the collective or the single-molecule dynamic properties of the pure system, as well as to sensitively characterize the composition of hydrogen-containing samples. Vice versa, the low mass values of the hydrogens (close to the neutron one) make these liquids very efficient moderators (through inelastic collisions) of the high energy neutrons produced by nuclear fission or spallation processes. At the same time, their range of liquid temperatures ($\simeq$20 K) is such that the final equilibrium energy distribution taking place in a hydrogen moderator is positioned in the so-called "cold" neutron range (1–10 meV). Therefore, liquid hydrogen and deuterium are extremely useful materials for the production of low energy neutrons, and have always been widely employed as cold neutron sources for condensed matter research.

It is important to note that although H_2 should be preferred as a moderator substance because of its lower mass, liquid (solid) deuterium is often chosen for the production of cold (ultracold) neutrons owing to its neutron absorption cross section, which is nearly three orders of magnitude lower than that of hydrogen. This is of particular importance in the attempt to obtain intense beams of cold neutrons. Indeed, absorption of a neutron by a nucleus grows by decreasing the neutron energy,

so use of a nuclide with a much lower absorption cross section, while increasing the overall beam flux, enhances particularly the flux of the least energetic neutrons. Therefore, as far as cold neutron production is concerned, such an important property makes D_2 at least as interesting as H_2, as shown, for example, by the choice of deuterium for the new cold source at the NIST Center for Neutron Research [7,8].

The still open questions regarding the structure and dynamics of these quantum liquids, our ability to predict their behavior, as well as the more technical aspects related to neutron moderation and production of increasingly intense cold neutron beams have therefore, as a common denominator, the same problem: reaching an accurate knowledge of some basic time correlation functions for H_2 and D_2 and, through these, being able to accurately reproduce the neutron scattering properties. Validation of a parameter-free algorithm for the computation of the neutron double differential cross section (DDCS) then not only becomes an important test of the dynamic structure factor used in the calculations, but also provides the possibility to build up neutron cross section libraries of the accuracy required at present in source design, without limitations either on the desired mapping of the kinematic plane, or on the initial neutron energy value E_0.

In a recent paper [9], in the following referred to as I, we started addressing the case of H_2 in equilibrium at liquid temperature (i.e., para-H_2) and proposed the use of quantum CMD simulations of the velocity autocorrelation function (VACF) to derive the single-molecule (*self*) center-of-mass (c.m.) dynamic structure factor $S_{\mathrm{c.m.,self}}(Q,E)$ through the Gaussian approximation (GA) [10,11]. This was done in an attempt to model at best the quantum effects that influence the dynamics of para-H_2 and that were not fully taken into account in existing models (see I, and references therein) for its DDCS. Proper consideration of the quantum nature of the system allowed us to show that no adjustable parameters were required to reach quantitative agreement with thermal and epithermal total cross section (TCS) data on an absolute scale, as well as with the few DDCS data available in absolute units. The same was found for the TCS at cold incident energies, where however also the *distinct* dynamics of para-H_2 must be considered along with the *self* one. The Sköld approximation for the modeling of the distinct part [12] that simply exploits the knowledge of $S_{\mathrm{c.m.,self}}(Q,E)$ and of the static structure factor $S_{\mathrm{c.m.}}(Q)$, was found to be sufficient to account very well for recent accurate TCS measurements in the cold range [13]. Nonetheless, the agreement found at cold-neutron incident energies turned out to be not as perfect as that obtained at thermal energies and above. For these reasons we hypothesized, among other possibilities, a slight failure of the Sköld approximation. This suggests we investigate more thoroughly the role of the distinct contributions and their schematization via the Sköld model. Between the two hydrogen liquids, D_2 is certainly the most appropriate system to refer to for this purpose, since its neutron scattering properties are such that both distinct (weighted by the coherent cross section only) and single-molecule (weighted also by the incoherent cross section) correlations are comparably highlighted by the neutron DDCS in a wide incident energy range, differently from para-H_2 where the incoherent cross section is huge, and distinct components in the DDCS become visible only when the incident neutrons have energies below the threshold of the first rotational transition, i.e., in the cold range.

This paper thus focuses on a treatment of the liquid D_2 case similar to the one proposed in I for para-H_2, with the further attempt to complete the verification of our quantum simulation-based algorithm for the calculation of the DDCS, and of its ability to faithfully describe, after double integration, the experimental TCS of both hydrogen liquids. Unfortunately, like in the para-H_2 case, properly corrected and normalized DDCS data are actually unavailable also for liquid deuterium, and quantitative comparisons with experiment can only be performed at the less detailed level of an integrated quantity like the TCS, for which only one data set at cold and thermal neutron energies seems to be available, i.e., that provided long ago by Seiffert [14]. Only very recently data in the ultracold neutron (UCN) range (below 10^{-3} meV) have been published [15] that we will take into consideration for comparison with future calculations. However, this requires a good modeling of the dependence of the scattering lengths on the incident energies, which is unnecessary outside the UCN range of energies.

In order to provide an additional check of the VACF predicted by the CMD quantum simulation method, here we also provide comparisons with the results obtained by means of RPMD computations. Determinations of $S_{\mathrm{c.m.,self}}(Q,E)$, i.e., the time Fourier transform of the intermediate scattering function $F_{\mathrm{c.m.,self}}(Q,t)$ obtained in the GA from the simulated VACF, will be synthetically indicated as CMD+GA and RPMD+GA, depending on the simulation method used to calculate the VACF.

The superiority of the quantum simulation based approach with respect to other models for the self-dynamics (see I), which cannot account properly for the "true" quanticity of the liquid, has been already demonstrated in I, and will not be further discussed here.

II. BRIEF REVIEW OF THE GENERAL FORMALISM

For diatomic homonuclear molecules, interacting through a substantially isotropic potential as the hydrogen one, the neutron DDCS in the sub-eV range can be approximated very well by that of free vibrorotors. In particular, it can be written as

$$\frac{d^2\sigma}{d\Omega dE} = \sqrt{\frac{E_1}{E_0}}S_{\mathrm{n}}(Q,E)$$

with [16]

$$S_{\mathrm{n}}(Q,E) = u(Q)S_{\mathrm{c.m.,dist}}(Q,E) + \sum_{J_0J_1v_1} F_{J_0J_1v_1}(Q)S_{\mathrm{c.m.,self}}(Q,E-E_{J_0J_1}-E_{0v_1}), \quad (1)$$

where the translational dynamics of the molecule is assumed to be fully decoupled from the intramolecular degrees of freedom, as evidenced above by the presence of the c.m. dynamic structure factors only. In Eq. (1), $S_{\mathrm{c.m.,dist}}(Q,E)$ and $S_{\mathrm{c.m.,self}}(Q,E)$ represent the distinct and self components of the total dynamic structure factor per molecule [see I, Eq. (2)], with $S_{\mathrm{c.m.}}(Q,E) = S_{\mathrm{c.m.,self}}(Q,E) + S_{\mathrm{c.m.,dist}}(Q,E)$.

The rotovibrational single-molecule structure is instead accounted for, in such hypotheses, by the second term on the right-hand side of Eq. (1), and corresponds to a sum of spectral lines centered at the energies of intramolecular rotovibrational ($J_0 \rightarrow J_1$, $v_0 \rightarrow v_1$) transitions, where the subscripts 0 and 1 are used to label initial and final state, respectively, of the rotational (J) and vibrational (v) quantum numbers. The ground vibrational state ($v_0 = 0$) is assumed here as the only one significantly populated in both hydrogen and deuterium at liquid temperatures. The function F depends on the quantum numbers and takes different expressions according to the nuclear spin statistics (i.e., it changes if the constituent nuclei are fermions or bosons) and on the ortho-para concentration, and contains both the coherent and incoherent nuclear cross sections [16]. Conversely, the weight of the intermolecular dynamics $u(Q)$ depends only on the coherent cross sections of the nuclei in the molecule, and, as the function F, on the wave vector Q exchanged in the scattering process.

Differently from the case of H_2 [9], the coherent and incoherent scattering lengths of the D nucleus have comparable values (6.674 and 4.003 fm, respectively). This implies that the distinct contributions to the neutron DDCS of D_2 are as important as the single-molecule ones for any relevant incident energy E_0 in the sub-eV range, which is a very different situation from that of para-H_2 where the intermolecular dynamics assumes a non-negligible role only at cold neutron energies. Thus, appropriate modeling of both $S_{\mathrm{c.m.,dist}}(Q,E)$ and $S_{\mathrm{c.m.,self}}(Q,E)$ is crucial in the deuterium case in a much wider E_0 range than in the case of para-H_2.

As stated in I, simple quantum simulation methods such as CMD and RPMD cannot reliably be used to evaluate time correlation functions that are not linear in position and momentum operators [2,3,17]. Unfortunately, this is precisely the case for the correlation functions entering the self and total intermediate scattering functions $F_{\mathrm{c.m.,self}}(Q,t)$ and $F_{\mathrm{c.m.}}(Q,t)$, so that also their spectra $S_{\mathrm{c.m.,self}}(Q,E)$ and $S_{\mathrm{c.m.}}(Q,E)$ cannot be determined directly by these methods. However, as far as the self-dynamics is concerned, it is possible to circumvent this problem while still accounting for the quantum behavior of the system, by using CMD or RPMD estimates of the c.m. VACF

$$u(t) = \langle \mathbf{v}_{\mathrm{c.m.}}(0) \cdot \mathbf{v}_{\mathrm{c.m.}}(t) \rangle, \tag{2}$$

in combination with the GA [10,11]. More details can be found in I. Briefly, the GA relates the VACF frequency spectrum ($\omega = E/\hbar$, with $2\pi\hbar$ Planck's constant)

$$p(\omega) = \frac{1}{2\pi} \int_{-\infty}^{\infty} dt e^{-i\omega t} u(t) \tag{3}$$

to $F_{\mathrm{c.m.,self}}(Q,t)$. In particular, it is assumed that

$$F_{\mathrm{c.m.,self}}(Q,t) \simeq e^{-Q^2\gamma_1(t)} \quad \text{for all } Q, \text{all } t \tag{4}$$

with

$$\gamma_1(t) = \frac{\hbar}{2M} \int_0^{+\infty} d\omega \, \frac{f(\omega)}{\omega} A(\omega). \tag{5}$$

In Eq. (5) $A(\omega)$ is given by

$$A(\omega) = [1 - \cos(\omega t)] \coth\left(\frac{\hbar\omega\beta}{2}\right) - i \sin(\omega t),$$

[$\beta = (k_B T)^{-1}$, with k_B as Boltzmann's constant] while $f(\omega)$ depends on the VACF spectrum according to

$$\begin{aligned} f(\omega) &= \frac{2M}{3\hbar\omega}[p(\omega) - p(-\omega)] \\ &= \frac{4M}{3\pi\hbar\omega} \int_0^{\infty} dt \sin(\omega t) \mathrm{Im}[u(t)]. \end{aligned} \tag{6}$$

By time Fourier transforming Eq. (4), a quantum determination of $S_{\mathrm{c.m.,self}}(Q,E)$ is thus achieved, and can be inserted in the DDCS algorithm implementing the intramolecular part of Eq. (1). As shown in I, the single-molecule dynamics obtained in this way fulfills very well the quantum second moment sum rule and provides TCS values in perfect agreement with experiment at all incident energies for which it completely dominates the scattering properties of para-H_2. On the basis of this, the CMD+GA results for $S_{\mathrm{c.m.,self}}(Q,E)$ are expected to provide an even better representation of D_2 self-dynamics, given the less pronounced quanticity of this (heavier) molecule.

Concerning the total dynamics, unfortunately no analogous way exists to derive a quantum-compliant $S_{\mathrm{c.m.}}(Q,E)$ from simulation of some linear-operator time correlation function, and from this to extract [by simple subtraction of the CMD+GA $S_{\mathrm{c.m.,self}}(Q,E)$] a quantum evaluation of the $S_{\mathrm{c.m.,dist}}(Q,E)$ needed to calculate the first term of Eq. (1). As we have shown in the case of para-H_2, a simple, yet effective, solution is to model the distinct dynamics through the Sköld approximation [12] that provides the total $S_{\mathrm{c.m.}}(Q,E) = S_{\mathrm{c.m.,self}}(Q,E) + S_{\mathrm{c.m.,dist}}(Q,E)$ as a suitable modification of its self part alone, namely

$$S_{\mathrm{c.m.}}(Q,E) \approx S_{\mathrm{c.m.}}(Q) S_{\mathrm{c.m.,self}}\left(\frac{Q}{\sqrt{S_{\mathrm{c.m.}}(Q)}}, E\right), \tag{7}$$

so that the distinct part of the dynamic structure factor is obtained as

$$\begin{aligned} S_{\mathrm{c.m.,dist}}(Q,E) \approx\ & S_{\mathrm{c.m.}}(Q) S_{\mathrm{c.m.,self}}\left(\frac{Q}{\sqrt{S_{\mathrm{c.m.}}(Q)}}, E\right) \\ & - S_{\mathrm{c.m.,self}}(Q,E), \end{aligned} \tag{8}$$

where $S_{\mathrm{c.m.}}(Q)$ is the c.m. static structure factor. In the present D_2 case, the $S_{\mathrm{c.m.}}(Q)$ determined by our neutron diffraction measurements [18] was employed. Of course, in the absence of experimental values, a valid alternative is to resort to PIMC determinations of $S_{\mathrm{c.m.}}(Q)$. Use of accurate data for the structure factor, along with a reliable quantum evaluation of $S_{\mathrm{c.m.,self}}(Q,E)$, was shown in I to be a sufficiently good method to account for the intermolecular terms contributing to the TCS of para-H_2 at cold incident energies and above. The same scheme was thus adopted for deuterium, providing an additional, more stringent, test of the effectiveness of such a crude approximation in total cross section calculations for both quantum liquids. This is indeed required to better understand the performance of the Sköld model, which is most likely responsible for the slightly inadequate description of the TCS of para-H_2 between 2 and 8 meV (see I).

III. QUANTUM SIMULATIONS OF THE VACF OF LIQUID D_2

In order to provide the appropriate input for our DDCS/TCS calculations, we have performed a series of CMD and RPMD simulations of liquid o-D_2 at $T = 20$ K and number density $\rho = 25.60$ nm^{-3} (i.e., on the experimental coexistence line [19]). Since, at that temperature, o-D_2 is in the rotational ground state, it was natural to model the intermolecular interactions by the same, spherically symmetric Silvera-Goldman pair potential [20] already used for p-H_2 in I. In fact, our CMD code was exactly that of part I, except that the molecular mass of H_2 was replaced by the D_2 one. The number of molecules in the cubical simulation box was usually $N = 256$, and the Trotter number $P = 64$, although with RPMD we have also performed additional simulations employing $N = 500$ and $P = 16$ and 32. The VACFs shown below are averages over ten independent runs, where, in the case of CMD, each single run consisted of 10^5 time steps of $\Delta t = 0.005$ ps (500 ps) in the isokinetic ensemble [21], while, for RPMD, the system was integrated for 10^6 time steps of $\Delta t = 0.001$ ps (1 ns) per run. Our implementation of CMD, which is basically classical molecular dynamics of the centroids (of the ring polymers replacing the quantum mechanical particles in the "classical isomorphism" [4]), in a quantum mechanical force field that is recalculated by short path integral Monte Carlo averages over the polymers' internal coordinates at each time step, has already been described in paper I.

In RPMD the classical isomorphism is taken literally, and the polymers internal modes are also propagated, on the time scale of intermolecular processes, by classical molecular dynamics [6]. This requires the introduction of fictitious monomer masses which are chosen equal to the mass of the original quantum particle, and, as a consequence, the polymers internal modes must be kept at a temperature PT (P being the number of momomers on a polymer). We have integrated the equations of motion of both the centroids *and* the monomers in real coordinates (although for the latter normal coordinates are more usual) using a set of $N + 1$ Gaussian thermostats [21,22]: a single global thermostat to keep the translational kinetic energy of the whole system of centroids at a value corresponding to the temperature T, and one thermostat each to keep the polymers "internal temperature" at PT. For the numerical integration we have again employed the leapfrog scheme in the simple variant of Brown and Clarke [23].

In CMD as well as in RPMD, time correlation functions were calculated up to a maximum time lag of 5 ps and tapered to zero at the end of this interval by a Welch window [24] when performing Fourier transforms or computing diffusion constants (see below).

In theory, the number of molecules N and the Trotter number P should be varied to ensure that the results of the simulations are close to both the thermodynamic and the quantum mechanical limit. We have verified that $N = 256$ and $P = 64$ are more than sufficient for the level of comparison with experimental data sought in the present paper. In particular, the Trotter number $P = 64$, which was chosen for consistency with our previous study of p-H_2, could have been lowered to $P = 32$ or even 16 without affecting the conclusions drawn below.

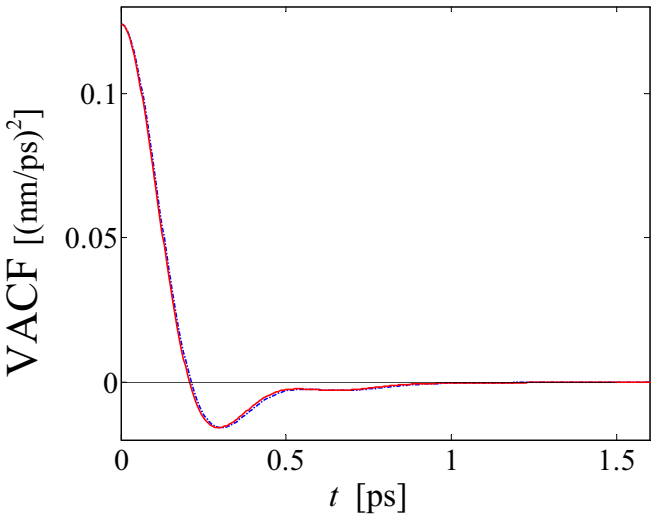

FIG. 1. Canonical velocity autocorrelation function $u_c(t)$ of deuterium at $T = 20$ K and $\rho = 25.60$ nm^{-3} obtained by means of the quantum CMD (blue dot-dashed curve) and RPMD (red solid curve) simulations described in the text.

The output of the quantum simulation is the canonical (or Kubo-transformed [25]) VACF:

$$u_c(t) = \frac{1}{\beta}\int_0^\beta d\lambda \langle e^{\lambda H}\mathbf{v}_{\text{c.m.}}(0)e^{-\lambda H}\cdot\mathbf{v}_{\text{c.m.}}(t)\rangle, \qquad (9)$$

where H is the Hamilton operator of the system. The canonical VACF is a real and even function of time, whose frequency spectrum

$$p_c(\omega) = \frac{1}{2\pi}\int_{-\infty}^{\infty} dt e^{-i\omega t}u_c(t) \qquad (10)$$

is related to the spectrum $p(\omega)$ of the VACF by the relation

$$p(\omega) = p_c(\omega)\frac{\beta\hbar\omega}{1-e^{-\beta\hbar\omega}}. \qquad (11)$$

Note that $p_c(\omega)$ is a real and even function of frequency, while $p(\omega)$ is a real, nonsymmetric spectrum, which satisfies the detailed balance condition $p(-\omega) = \exp(-\beta\hbar\omega)p(\omega)$.

Figure 1 reports our CMD and RPMD simulation results for the VACF of D_2. The two curves are very similar, suggesting that both methods can effectively be used to simulate such a correlation function. Given the results obtained in I for para-H_2 using the CMD VACF, we expect then, in the present D_2 case, a successful performance of both the CMD and RPMD methods, although these involve quite different approximations of the exact quantum dynamics, as interestingly discussed in Refs. [26,27].

By means of the equations given in Sec. II we calculated the corresponding $\gamma_1(t)$, whose real and imaginary parts are shown in Fig. 2. Both functions tend to linear behavior in a very short time. A slight difference in the asymptotic limit of Re $[\gamma_1(t)]$ as obtained by RPMD and CMD can be detected. This implies that the two methods predict slightly different values of the self-diffusion coefficient D (present values are 3.5×10^{-9} m^2 s^{-1} for CMD, 3.4×10^{-9} m^2 s^{-1} for RPMD) [28], though both are well within the uncertainty on the experimental value at 20 K, $D = (3.7 \pm 0.4) \times 10^{-9}$ m^2 s^{-1}

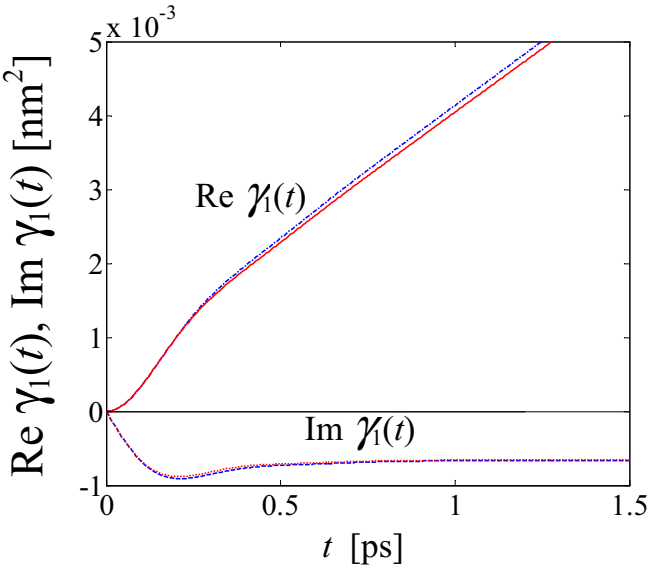

FIG. 2. Real and imaginary parts of $\gamma_1(t)$ as derived from CMD (dot-dashed and dashed blue curves) and from RPMD (solid and dotted red curves) simulations of the VACF of D_2 at $T = 20$ K and $\rho = 25.60\ \mathrm{nm}^{-3}$.

[29]. The present D_2 results confirm that CMD and RPMD exhibit similar performances close to the triple point, as shown by Pérez *et al.* [30] for the hydrogen case also by means of general criteria that do not resort to comparison with experimental data but give important indications on the quality of the results. Another experiment-independent way to assess the quality of the approximate Kubo-transformed correlation functions obtained by RPMD has also been recently discussed in Ref. [31]. However, as for mean kinetic energies in liquid hydrogens, it seems that CMD is able to provide slightly more accurate results than RPMD (see, e.g., [32]).

In our case the small difference in D does not significantly affect the resulting self-DDCS spectra, as shown, for an example incident energy E_0 of 10 meV and for various scattering angles θ, in Fig. 3. CMD and RPMD neutron spectra obtained in the GA for the second term of Eq. (1) are virtually indistinguishable at all scattering angles, and we verified that this is the case even at other E_0 values and scattering angles. In particular, differences between the two outputs are well below the errors typically affecting measured quantities, so that a comparison with experiment cannot discriminate between the two and, in this respect, the two simulation methods turn out to be equivalent. Note how in the right panel of Fig. 3 the spectra are, as expected, visibly shifted due to recoil. Finally, it is important to specify that our DDCS calculations have been performed for D_2 in equilibrium at the given temperature, corresponding approximately to a 98% concentration of ortho-molecules.

IV. TOTAL CROSS SECTION RESULTS

As mentioned, it is not to be expected that self-calculations alone can account for the scattering properties of D_2, due to the non-negligible coherent contribution that enhances the effect of the distinct intermolecular correlations present in the first term of Eq. (1). Nonetheless, it is crucial to have reliable and quantum-compliant determinations of $S_{\mathrm{c.m.,self}}(Q,E)$ as the starting point of any attempt to describe the total dynamics of D_2 and, thereby, the measured neutron cross section.

As shown in Fig. 4, self-calculations expectedly miss an appropriate description of the D_2 TCS data [14] in the whole experimental range. A considerable overestimate is indeed observed, requiring the introduction of the additional (negative) distinct component.

Despite the drastic simplifications inherent to the Sköld approximation, the corresponding results, also shown in Fig. 4, turn out to be surprisingly good, provided that accurate, either experimental or simulated, information on liquid D_2 static structure is used, as in the present case [18]. In particular, the CMD+GA (or RPMD+GA) plus Sköld combination reproduces rather well the shape and height of the peak centered at about 3.5 meV. Unfortunately measured data are provided without any indication about the errors. However,

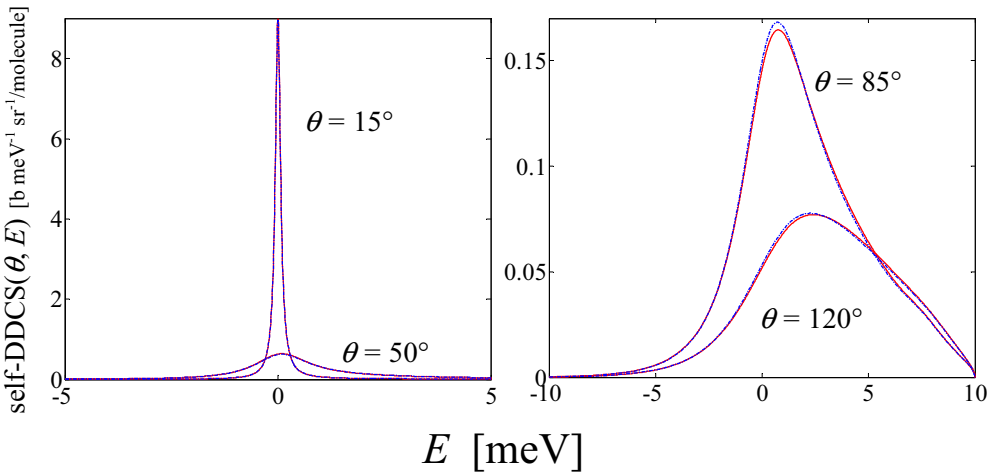

FIG. 3. Self part [second term of Eq. (1)] of the double differential cross section per molecule of liquid D_2 at $T = 20$ K and $\rho = 25.60\ \mathrm{nm}^{-3}$, as a function of the exchanged energy E, at some example scattering angles θ. The CMD+GA (blue dot-dashed curves) and RPMD+GA (red solid curves) results are equivalent, as far as a possible comparison with experimental data is concerned.

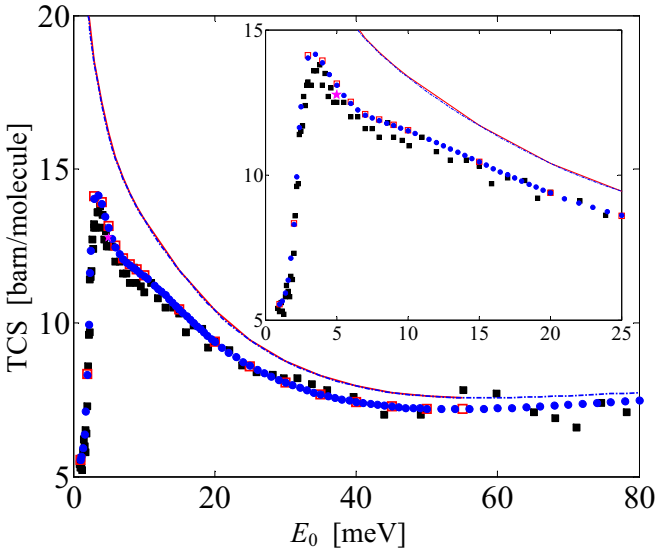

FIG. 4. Total scattering cross section of liquid D_2 at cold and thermal energies, as measured by Seiffert (black squares) at 19 K [14]. The CMD+GA (blue dash-dotted line) and RPMD+GA (red solid line) self calculations expectedly overestimate the experimental data. The addition of a distinct contribution, as provided by the Sköld model, leading to the blue full circles and red empty squares in the CMD+GA and RPMD+GA case, respectively, brings the computed TCS in good agreement with the experimental data. The inset focuses on the cold and subthermal range of incident energies. The pink star at $E_0 = 5$ meV corresponds to the TCS value for *normal* D_2.

the residual deviations (apparently a small constant offset, better detectable in the inset of Fig. 4 between 5 and 15 meV) from the experimental cross section, are difficult to ascribe to inaccuracies of the simulations, and in addition require us to exclude the possible occurrence of slight systematic errors in Seiffert data [14]. Also, the difference in temperature between Seiffert measurements and our calculations is small enough to exclude temperature effects and their visibility at the level of the TCS, since, for instance, it is well known that structural changes are extremely limited with varying temperature in high density liquids [33]. Conversely, a brief test calculation performed at $E_0 = 5$ meV reveals that the offset from Seiffert data is halved if the *normal* D_2 ortho-to-para concentration is considered in place of the equilibrium one. Unfortunately, no information about the duration of the measurements and the conversion of D_2 is given in Ref. [14], differently from the case of the hydrogen data. Concerning the remaining minor differences in TCS, we cannot exclude that they might be the signature of an imperfect description of the distinct dynamics of a quantum liquid, as discussed in the next section. Nonetheless, it would be useful that new TCS data become available for liquid D_2 too, with appropriate estimates of the experimental uncertainties and with a good knowledge of the sample concentrations, as recently done for para-H_2 by Grammer and co-workers [13].

V. DDCS RESULTS

As stated in the Introduction, experimental $S_n(Q,E)$ data for liquid D_2 have been provided only in arbitrary units (e.g., [34,35]), preventing us from a quantitative validation of our DDCS outputs [the simple relation between DDCS and $S_n(Q,E)$ was given before Eq. (1) in Sec. I]. It is anyway significant and informative to preliminary probe the quality of the present method also in predicting the spectral line shapes, independently from the absolute-scale values. In Fig. 5 we report the comparison of our calculated spectra (CMD+GA+Sköld) at several Q values of the three-axis neutron measurements performed at $E_0 = 34.95$ meV on *normal* D_2 at 20.14 K by Bermejo and co-workers [34]. For consistency with the results presented there, new constant-Q DDCS calculations have been performed appositely for normal D_2. Measured data were more reliably read off from Fig. 4 of the quoted paper, although they are given without error bars, an idea of which, at some Q values, can be deduced from Fig. 5 of the same paper. Our absolute-normalized data have been convoluted with the resolution function $R(E)$ of the measurements, and then multiplied by an arbitrary factor to bring the two data sets on the same scale.

At Q values above 10 nm^{-1}, measurements and calculations are in very good agreement, and particularly at the main peak position $Q_p = 20$ nm^{-1} of the static structure factor. Indeed, at Q_p, where collective modes in simple liquids are typically overdamped and propagation tends to arrest (see, e.g., [36] and Fig. 9 of Ref. [37]), a bell-shaped curve of appropriate integral and with no inelastic features (like the Sköld one) suites a realistic representation of the distinct dynamics. Conversely, at and below 10 nm^{-1}, differences show up, which increase with decreasing Q. However, discrepancies cannot be explained only in terms of the presence of underdamped modes in the fluid (with related inelastic peaks in the spectrum) and expectedly missed by the Sköld schematization. In fact, a word of caution is due before interpreting the data at 8 and 10 nm^{-1}. In this respect, we note that the mentioned arbitrary scale factor takes the values 55.4, 54.9, 36.8, 36.0, 36.1, 36.8 at the increasing Q values of Fig. 5, respectively, with an abrupt variation between 10 and 14 nm^{-1}. Since the use of the Sköld model, in combination with a reliable $S_{c.m.}(Q)$, does not affect the correctness of the integrated intensity, this suggests that the measurements or the experimental data analysis may have been more critical at low Q, where the normalization factor inexplicably changes (by 60%), but the largest discrepancies in shape are also found at the same time.

We conclude, therefore, that the comparison between spectral shapes is fully satisfactory for the majority of the investigated Q's. At smaller Q values, instead, it is difficult to find out the origin of the jump in the normalization factor and to confidently attribute problems either to calculations or to experiment. We can only state that the absolute-scale outputs of the DDCS code do not present discontinuities with increasing Q, and are consistent, in integrated intensity, with the growth of the static structure factor. Anyway, such an ambiguity prevents one from any useful conclusion about the more or less effective performance of the Sköld model in the low-Q range, and calls definitely for new inelastic neutron scattering experiments, aimed also at a quantitative absolute-scale determination of the DDCS in well-controlled sample concentration conditions. On the other hand, for TCS calculation purposes, we can rely on the fact that, beyond a detailed spectral shape description

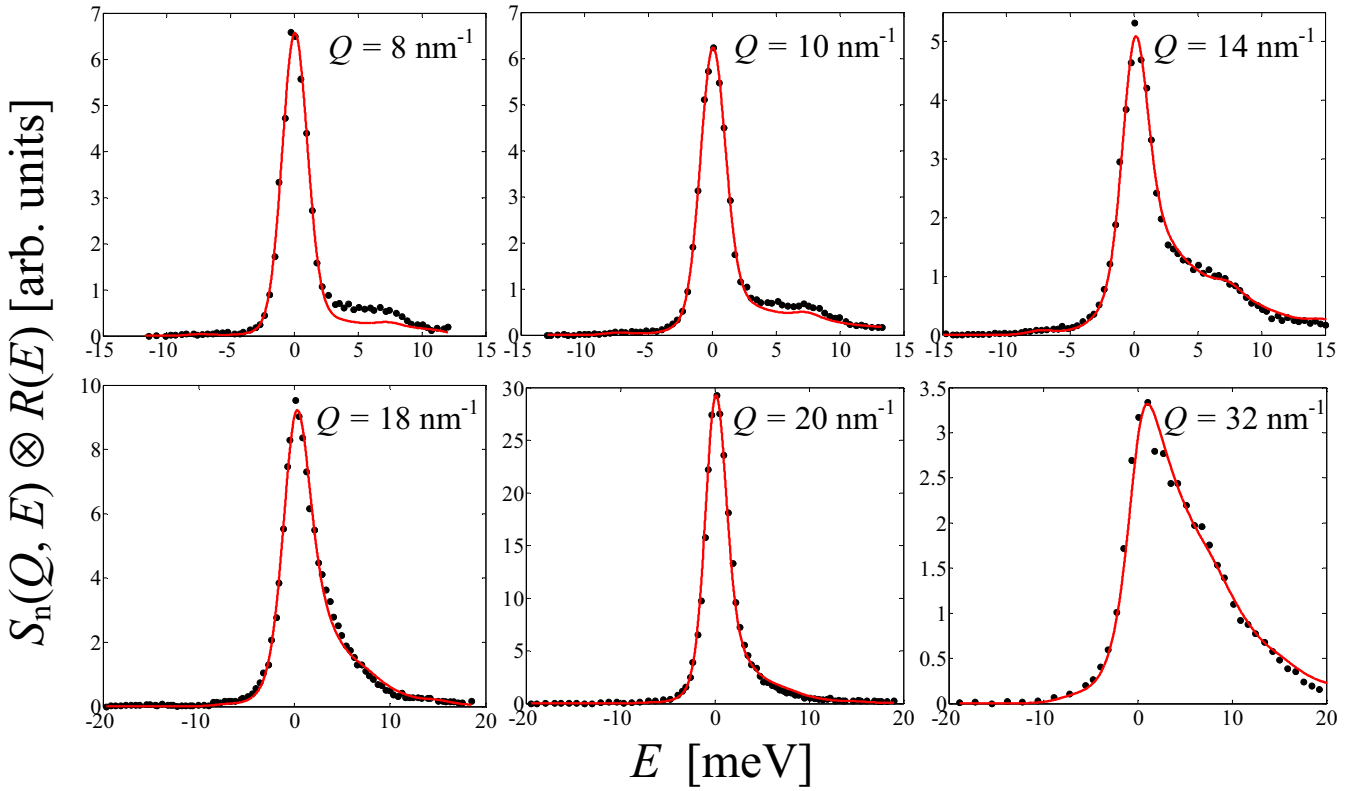

FIG. 5. Liquid normal D_2 spectra as obtained by inelastic neutron scattering three-axis measurements [34] (black dots without error bars) and present calculations in the CMD+GA+Sköld schematization (red solid curve).

at whatever Q, computations ensure a realistic energy integral of the DDCS.

VI. CONCLUDING REMARKS

We have shown that CMD and RPMD quantum simulations provide comparable results for the VACF of liquid D_2. The c.m. self-dynamic structure factor obtained in the GA from either of the two methods can then be used as the starting point for attempts to describe the neutron scattering properties of this quantum liquid. A simple description for the distinct dynamics, such as the Sköld model, is found, like in para-H_2, to account rather well for the total scattering of D_2, provided it is combined with "first-principle" calculations of the self-DDCS, based on the only hypotheses that both the chosen intermolecular potential and the decoupling among translations, rotations, and vibrations, permit an appropriate description of the D_2 response to neutrons in the sub-eV range. Our quantum simulation based method proves accurate and flexible enough for the setting up of neutron DDCS databases, useful in important applications of both hydrogen liquids. In particular, the present capability to predict the DDCS without other inputs, except for the temperature and density, the corresponding VACF, and the molecular parameters of these molecules, may be extremely useful in determining the performance of D_2 neutron moderators. The results presented here and in paper I suggest that further studies should be devoted to the determination of the collective dynamics of both liquids, not only by means of inelastic neutron scattering measurements, but also through advancements in the field of quantum simulation techniques, by developing methods able to allow direct access to the total dynamics in a more reliable way than through the Sköld recipe. In this respect, quantum simulation algorithms such as the one very recently proposed in Ref. [38] as a modification of the Feynman-Kleinert linearized path integral method [39], might represent a promising improvement worthy of further research and experimental verification.

ACKNOWLEDGMENTS

E.G. gratefully acknowledges the welcome and nice interaction with the whole staff of the Institut Laue Langevin during her 2014 work in Grenoble on the neutron cross sections of cryogenic liquids.

[1] M. P. Allen and D. J. Tildesley, *Computer Simulations of Liquids* (Clarendon, Oxford, 1987).
[2] J. Cao and G. A. Voth, J. Chem. Phys. **100**, 5106 (1994).
[3] S. Jang and G. A. Voth, J. Chem. Phys. **111**, 2371 (1999).
[4] D. Chandler and P. G. Wolynes, J. Chem. Phys. **74**, 4078 (1981).

[5] D. Chandler, J. Phys. Chem. **88**, 3400 (1984).

[6] I. R. Craig and D. E. Manolopoulos, J. Chem. Phys. **121**, 3368 (2004).

[7] R. E. Williams, M. Middleton, P. Kopetka, J. M. Rowe, and P. C. Brand, A Liquid Deuterium Cold Neutron Source for the NIST Research Reactor—Conceptual Design, Proceedings of the IGORR Conference 2013, Daejeon, South Korea, 2013, available at http://www.igorr.com/home/liblocal/docs/IGORR2013/07_1003.pdf.

[8] Z. Wu, R. E. Williams, and S. O'Kelly, Preliminary Studies on a New Research Reactor and Cold Neutron Source at NIST, Proceedings of the IGORR 2014/IAEA Technical Meeting, Bariloche, Argentina, 2014, available at https://www.ncnr.nist.gov/staff/zeyun.wu/papers/Wu_IGORR2014.pdf.

[9] E. Guarini, M. Neumann, U. Bafile, M. Celli, D. Colognesi, E. Farhi, and Y. Calzavara, Phys. Rev. B **92**, 104303 (2015).

[10] G. H. Vineyard, Phys. Rev. **110**, 999 (1958).

[11] A. Rahman, K. S. Singwi, and A. Sjölander, Phys. Rev. **126**, 986 (1962).

[12] K. Sköld, Phys. Rev. Lett. **19**, 1023 (1967).

[13] K. B. Grammer *et al.*, Phys. Rev. B **91**, 180301(R) (2015).

[14] W. D. Seiffert, Euratom Report No. EUR 4455d (1970), available at https://www.google.it/?gfe_rd=cr&ei=TgRTV6DXDoyA8Qen9IyIDw&gws_rd=ssl#q=EUROP%C3%84ISCHE+ATOMGEMEINSCHAFT+EURATOM+wasserstoff%2C+deuterium+THERMISCHE+NEUTRONEN; W. D. Seiffert, B. Weckermann, and R. Misenta, Z. Naturforsh **25**a, 967 (1970), available at http://zfn.mpdl.mpg.de/data/Reihe_A/25/ZNA-1970-25a-0967.pdf.

[15] S. Döge, C. Herold, S. Muller, C. Morkel, E. Gutsmiedl, P. Geltenbort, T. Lauer, P. Fierlinger, W. Petry, and P. Boni, Phys. Rev. B **91**, 214309 (2015).

[16] E. Guarini, J. Phys.: Condens. Matter **15**, R775 (2003).

[17] T. D. Hone and G. A. Voth, J. Chem. Phys. **121**, 6412 (2004).

[18] M. Zoppi, U. Bafile, E. Guarini, F. Barocchi, R. Magli, and M. Neumann, Phys. Rev. Lett. **75**, 1779 (1995).

[19] H. M. Roder, G. E. Childs, R. D. McCarty, and P. E. Angerhofer, Survey of the Properties of the Hydrogen Isotopes Below Their Critical Temperatures, National Bureau of Standards Technical Q Note 641 (1973), available at https://archive.org/details/surveyofproperti641rode; https://ia801605.us.archive.org/32/items/surveyofproperti641rode/surveyofproperti641rode.pdf.

[20] I. F. Silvera and V. V. Goldman, J. Chem. Phys. **69**, 4209 (1978).

[21] D. J. Evans and G. Morriss, *Statistical Mechanics of Nonequilibrium Liquids*, 2nd ed. (Cambridge University Press, Cambridge, 2008).

[22] W. G. Hoover, *Computational Statistical Mechanics* (Elsevier, Amsterdam, 1991).

[23] D. Brown and J. H. R. Clarke, Mol. Phys. **51**, 1243 (1984).

[24] W. H. Press, S. A. Teukolsky, W. T. Vetterling, and B. P. Flannery, *Numerical Recipes in FORTRAN, The Art of Scientific Computing*, 2nd ed. (Cambridge University Press, Cambridge, 1992).

[25] R. Kubo, Rep. Prog. Phys. **29**, 255 (1966).

[26] S. Jang, A. V. Sinitskiy, and G. A. Voth, J. Chem. Phys. **140**, 154103 (2014).

[27] T. J. H. Hele, M. J. Willatt, A. Muolo, and S. C. Althorpe, J. Chem. Phys. **142**, 191101 (2015).

[28] These are the values obtained with $P = 64$ and $N = 256$ molecules from CMD and $N = 500$ molecules from RPMD, but we note that the diffusion constant increases/decreases slightly with the number of molecules/Trotter number.

[29] D. E. O'Reilly and E. M. Peterson, J. Chem. Phys. **66**, 934 (1977).

[30] A. Pérez, M. E. Tuckerman, and M. H. Müser, J. Chem. Phys. **130**, 184105 (2009).

[31] L. H. de la Peña, Phys. Chem. B **120**, 965 (2016).

[32] T. D. Hone, P. J. Rossky, and G. A. Voth, J. Chem. Phys. **124**, 154103 (2006).

[33] E. Guarini, F. Barocchi, R. Magli, U. Bafile, and M. C. Bellissent-Funel, J. Phys.: Condens. Matter **7**, 5777 (1995).

[34] F. J. Bermejo, F. J. Mompeán, M. García-Hernández, J. L. Martínez, D. Martin-Marero, A. Chahid, G. Senger, and M. L. Ristig, Phys. Rev. B **47**, 15097 (1993).

[35] M. Mukherjee, F. J. Bermejo, B. Fåk, and S. M. Bennington, Europhys. Lett. **40**, 153 (1997).

[36] M. Sampoli, U. Bafile, F. Barocchi, E. Guarini, and G. Venturi, J. Phys.: Condens. Matter **20**, 104206 (2008).

[37] E. Guarini *et al.*, Phys. Rev. B **88**, 104201 (2013).

[38] K. K. G. Smith, J. A. Poulsen, G. Nyman, A. Cunsolo, and P. J. Rossky, J. Chem. Phys. **142**, 244113 (2015).

[39] J. A. Poulsen *et al.*, J. Chem. Theory Comput. **2**, 1482 (2006).